JOURNAL OF GEOPHYSICAL RESEARCH, VOL. 108, NO. D1, 8155, doi:10.1029/2001JD000443, 2003

Seasonal and decadal patterns of soil carbon uptake and emission along an age sequence of burned black spruce stands in interior Alaska

Katherine P. O'Neill,[1,3] Eric S. Kasischke,[2,4] and Daniel D. Richter[1]

Received 6 February 2001; revised 25 October 2001; accepted 27 October 2001; published 15 January 2003.

[1] Postfire changes in the local energy balance and soil chemistry may significantly alter rates of carbon turnover in organic-rich soils of boreal forests. This study combines field measurements of soil carbon uptake and emission along a 140-year chronosequence of burned black spruce stands to evaluate the timescales over which these disturbance effects operate. Soil CO_2 efflux increased as a function of stand age at a mean rate of 0.12 Mg C ha^{-1} yr^{-2} up to a maximum of 2.2 Mg C ha^{-1} yr^{-1} in the 140-year-old stand. During this same time period, organic soil horizons sequestered carbon and nitrogen at rates of 0.28–0.54 and 0.0076 Mg N ha^{-1} yr^{-1}, respectively. A mass balance model based on field measurements suggests that postfire changes in root and microbial respiration caused these soils to function as a net source of carbon for 7–15 years after fire, releasing between 1.8 and 11.0 Mg C ha^{-1} to the atmosphere (12.4–12.6% of total soil organic matter). These estimates are on the same order of magnitude as carbon losses during combustion and suggest that current models may underestimate the effect of fire on carbon emissions by a factor of 2. *INDEX TERMS:* 1851 Hydrology: Plant ecology; 1699 Global Change: General or miscellaneous; *KEYWORDS:* fire, carbon, nitrogen, soil, chronosequence, mass balance model

Citation: O'Neill, K. P., E. S. Kasischke, and D. D. Richter, Seasonal and decadal patterns of soil carbon uptake and emission along an age sequence of burned black spruce stands in interior Alaska, *J. Geophys. Res.*, *108*(D1), 8155, doi:10.1029/2001JD000443, 2003.

1. Introduction

[2] The soils of boreal forest ecosystems have one of the highest carbon densities in the world and are estimated to contain between one-quarter and one-third of all soil carbon (200–7500 Gt C) [*Gorham*, 1991; *Dixon et al.*, 1994]. For much of the last 15,000 years, harsh winter temperatures, annual moisture deficits, and permanently frozen soils have limited rates of decomposition, resulting in thick accumulations of organic matter on the forest floor. In the Alaskan interior, the highest rates of soil carbon storage are associated with black spruce stands, which are noted for their low productivity and reduced rates of nutrient cycling [*MacLean et al.*, 1983]. The combination of cold temperatures, saturated surface horizons, and low litter quality all limit the decomposition of litter- and moss-derived organic material in these systems, resulting in large accumulations of carbon and nutrients in the organic layers of the profile. In boreal forests of northern Canada, mature black spruce–feathermoss stands have been found to sequester carbon at rates of 0.1–0.3 Mg C ha^{-1} yr^{-1} [*Harden et al.*, 1997]. Current estimates suggest that northern soils (forest and peatland) may function as a net carbon sink on the order of 0.70 Gt yr^{-1} [*Apps et al.*, 1993].

[3] On an ecosystem level, one of the primary factors regulating patterns of carbon storage and release in northern landscapes is wildfire [*Kasischke et al.*, 1995, 2000a, 2000b]. In addition to the immediate loss of carbon during combustion, postfire changes in soil temperature, moisture, and chemistry have the potential to enhance rates of decomposition following fire and release large amounts of stored carbon to the atmosphere [*Richter et al.*, 2000; *Auclair and Carter*, 1993; *Burke et al.*, 1997; *Bonan and Van Cleve*, 1991; *Van Cleve and Yarie*, 1986; *Flanagan and Van Cleve*, 1977]. Since these carbon losses are not immediately balanced by an uptake of carbon in NPP, these enhanced rates of decomposition represent a net loss of carbon from the ecosystem in the first years after fire. Over longer timescales, however, mobilization of soil nutrients caused by melting permafrost, ash deposition, and changes in soil thermal and moisture regimes may create more favorable conditions for plant growth and result in increased NPP and carbon inputs to the soil [*MacLean et al.*, 1983; *Viereck et al.*, 1983]. Ultimately, the ecological significance of carbon losses during combustion and postfire decomposition depends upon the timescales over which these

---

[1] Nicholas School of the Environment, Duke University, Durham, North Carolina, USA.

[2] ERIM International, Inc., Ann Arbor, Michigan, USA.

[3] Now at North Central Research Station, USDA Forest Service, St. Paul, Minnesota, USA.

[4] Now at Department of Geography, University of Maryland, College Park, Maryland, USA.

0148-0227/03/2001JD000443$09.00

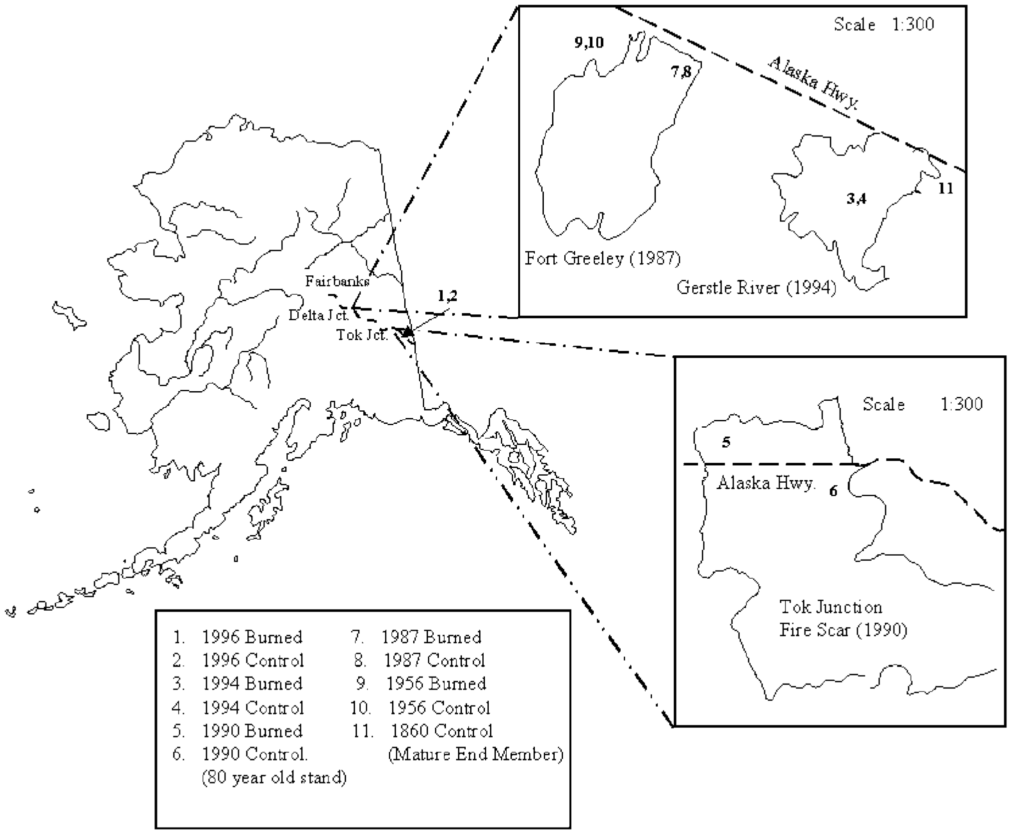

Figure 1. Site location map. Inset maps show boundaries of burn scars. The control stand for the 1990 burn was also used as the 80-year-old stand in the chronosequence.

communities recover from disturbance and the balance between carbon losses and inputs in the years and decades following fire.

[4] Over millennial timescales, northern soils have come into a dynamic equilibrium with fire disturbance. Increased decomposition following fires releases nutrients immobilized in mosses and slowly decomposing organic horizons, making them available for uptake in new tree and shrub biomass. However, this increased decomposition can not persist for very long because, over geologic time, northern soils have been a net sink for carbon; that is, the amount of carbon released during and after fires has been more than balanced by the amount of carbon stored in the years between fire disturbance [*Harden et al.*, 1997, 2000]. However, under a global warming scenario, both surface temperatures and summer droughts are expected to increase in northern latitudes, potentially altering both the frequency and the severity of wildfires [*Wotton and Flannigan*, 1993; *Stocks et al.*, 2000]. Understanding the potential magnitude and duration of postfire disturbance effects on the soil carbon balance is critical to developing models of ecosystem response to climate-driven changes in fire regime.

[5] This paper combines field measurements of soil CO_2 efflux and carbon storage along a 140-year age sequence of burned black spruce stands with a mass balance model of carbon accumulation to address the following questions: (1) how do rates of carbon sequestration and emission change in the years to decades following fire, (2) to what extent does fire convert upland black spruce systems from a net sink to a net source of carbon, (3) over what timescales might this potential carbon source persist, and (4) how might northern soils respond to potential increases in fire frequency.

2. Site Description

[6] Studies were conducted along a chronosequence of burned black spruce stands located in the eastern Tanana River Valley between the towns of Delta Junction and Tetlin Junction, Alaska (Figure 1 and Table 1). The time since last fire was determined by historical record for recent burns and by tree ring analysis for more mature stands; stand ages were 1, 3, 7, 10, 41, 80, and 140 years (using 1997 as a base year). All of the "recent" fire scars (the 1, 3, 7, 10, and 41 year old stands) had a burn boundary that resulted from a nonnatural feature (e.g., a road or fire break) allowing us to identify an unburned, mature black spruce stand as a control that was comparable to the preburn vegetation structure and stand density of the burned stands. The age of the control stands ranged from 80 to 160 years. An additional 140-year-old black spruce stand was selected as a mature end-member for the chronosequence. Due to the logistical difficulty of locating comparable black spruce stands that last burned between 50 and 150 years ago, the control for the 7-year-old burn was also used as the 80-year-old stand in the chronosequence.

[7] To evaluate the effects of time on soil developmental processes, the chronosequence approach requires accurate

Table 1. Location and Description of Study Sites

Year of most recent fire	Location	Fire status	Site code	Soil series	Soil classification	Depth of maximum seasonal thaw (cm)
1996	Tetlin Junction	Burned	B96	–	–	70.56 ± 0.68
		Control	UB96			16.05 ± 0.62
1994	Hajdukovich Creek	Burned	BHC	Volkmar silt loam	Coarse–silty, mixed, nonacid Aeric Cryaquept	>100
		Control	UBHC			20.10 ± 1.14
1990	Tok Junction	Burned	B90	–	Coarse–silty, mixed, nonacid Pergelic Cryaquept	>100
		Control	UB90			22.91 ± 2.35
1987	Delta Junction	Burned	B87	Nenana silt loam	Coarse–silty over sandy–skeletal, mixed typic Cryrochrept	>100
		Control	UB87			40.25 ± 1.57
1956	Ft. Greeley	Burned	B56	–	–	–
		Control	UB56		–	–
≈1855	Gerstle River	Control	UB140	Saulich silt loam	Loamy, mixed, nonacid Histic Pergelic Cryaquept	23.3 ± 0.74

The control stand for the 7-year-old fire scar was also used as the 80-year-old stand in the chronosequence. The 140-year-old stand represents a mature end-member and does not have a separate control. Dashed lines indicate that no soil series have been described. Maximum depth of thaw determined as the mean ± 1 s.e. of 10 measurements made at each plot in late August 1997.

ages for soil surfaces, low intrasite and intersite variability, and identification of appropriate end-members. Sampling sites were limited to black spruce stands with soils of similar texture, drainage class, ground vegetation, and slope position. However, potential differences in burn severity need to be taken into consideration when interpreting data from the chronosequence. Detailed measurements of burn severity in the 1990 fires near Tok Junction (7-year-old stand) by *Kasischke et al.* [2000a] indicate that black spruce stands were burned by a combination of ground and crown fires that released an average of 33.5 tC ha^{-1} (range 13.6–75.7 tC ha^{-1}). Visual surveys indicated that fires in the 1, 3, and 10 year old stands included both ground and crown fires (e.g., virtually 100% mortality and almost 100% of understory vegetation consumed by fires), with 30–40% of burned canopy vegetation similar to that of the 7-year-old stand. However, the ground fire in the 1-year-old stand appeared to be less severe than at other chronosequence stands, as evidenced by the 25–30 cm of organic material remaining on the forest floor. Due to the amount of vegetation regrowth and forest floor development, it was not possible to determine burn severity in stands older than 10 years.

[8] Soils consisted of level to moderately sloping well-drained silt loams over gravel or sand located on outwash plains or terraces. Mature black spruce stands are characterized by highly developed organic profiles that overlie the mineral soils that were classified as coarse–silty, mixed, nonacid Aeric Cryaquepts and coarse–silty over sandy–skeletal, mixed, Typic Cryochrepts [*Schoephorster*, 1973]. Since mature stands typically remain frozen within a meter of the surface, these soils would be reclassified as Gelisols under the 8th edition of Soil Taxonomy [*USDA NRCS*, 1998]. Nomenclature for organic soil horizons follows that of the Canadian Soil Classification System [*Agriculture Canada*, 1987]. The upper portion of the organic profile (O_f or fibric horizon) is composed of relatively undecomposed mosses and moss litter. The botanical origin of these materials is still recognizable with the unaided eye and soils contain more than 40% rubbed fiber content. The lower part of the soil profile (O_h or humic horizon) consists of highly decomposed and charred materials that have accumulated over decades to millennia. The botanical origin of humic materials cannot be visually determined and the rubbed fiber content is less than 10% by volume. Materials of intermediate decomposition that have been physically and chemically altered, yet do not meet the requirements for either a fibric or a humic horizon are classified as mesic (O_m).

[9] The Alaskan interior between the Alaska and Brooks Mountain Ranges experiences a strong continental climate characterized by moderate temperatures and precipitation during the summer months (May–August) and exceedingly cold and dry conditions during the winter. Average maximum and minimum annual temperatures in Tok Junction (1954–1998) are 2.2°C and −10.1°C, respectively, with lowest temperatures occurring in January (mean $-27.0 \pm 11.6_{s.d.}$ °C) and highest temperatures in July (mean $14.4 \pm 16.1_{s.d.}$ °C). Annual precipitation averages $23.4 \pm 7.5_{s.d.}$ cm; one-third of this total falls as snow during October–March and one-third as rain in July and August National Weather Service, Alaska region (data available at http://www.wrcc.dri.edu/summary/climsmak.htm, 2000). Because the study sites extended across a distance of 220 km, stands near the northern edge of the study area are approximately 2°C warmer than stands to the south and receive 6 cm of additional precipitation per year [National Climatic Data Center, 2000]. Although these differences in microclimate introduce additional variability among the study sites, the magnitude of these differences is relatively small and may even be considered negligible on an annual or monthly basis. The present fire cycle for Alaskan boreal forests ranges from 90 to 360 years (E. S. Kasischke et al., Fire trends in the Alaskan boreal forest region, manuscript in review, 2001, with the frequency for the study region being on the order of 150 years. Recovery of the forest to preburn status may take 100 years or longer. The fire season runs from April to September, with the greatest number of fires occurring during June and August.

3. Methods

3.1. Soil CO_2 Efflux

[10] Within each burned and control stand, 10 sampling points were located in two parallel rows spaced 10-m apart along 50 × 30-m grids. At each sampling point, CO_2 emissions from the surface of the forest floor were measured with a dynamic closed gas exchange system consisting of a nondispersive infrared analyzer (EGM-1 environmental gas

monitor, PP Systems) coupled with an opaque sampling chamber (SRC-1). A detailed description of this system and its operation is likewise given by *Parkinson* [1981]. CO_2 concentration (ppmv) within the chamber was measured at 8-s intervals over a maximum 2-min period and the rate of increase used to calculate flux (g CO_2 m^{-2} hr^{-1}). Care was taken to ensure that initial CO_2 concentration was at or below atmospheric levels ($\approx$360 ppmv). Living moss and vegetation were not removed prior to measurement in order to limit site disturbance and the subsequent potential for enhanced decomposition and disturbance of root biomass; thus, respiration from living mosses is included as a part of soil efflux. Measurements were made weekly during the growing season from May to mid-September 1997. Statistical analyses of data were based upon the mean of the 10 measurements collected within each stand for a given sampling period. Concurrent with each CO_2 measurement, soil temperature was measured at 10 and 20 cm below the surface of the moss layer/forest floor.

3.2. Carbon and Nitrogen Content of Soil Horizons

[11] Within four burned and four control plots, 10 40-cm^2 soil cores were excavated at randomly located sampling points (n = 40 burned cores and 40 control cores) using a shovel and/or saw and subdivided into genetic horizons (moss, fibric, and humic). Two cubes were cut from the center of each horizon using an electric knife with two reciprocating blades; this method minimized the potential of compaction. Cube dimensions were measured to the nearest 0.1 cm and the samples weighed, dried in a 65°C oven for 48 hours, and then reweighed to determine volumetric moisture content and bulk density. Oven-dried samples were ground in a Wiley Mill until all material was able to pass through a 60-mesh sieve. Fine roots that passed through the sieve were not removed prior to grinding. Total percent C and N were measured by combustion on a Perkins Elmer 2400 Series II CHNS/O Analyzer.

3.3. Percent Cover of Understory Vegetation

[12] At each site, percent cover estimates for species in the understory and ground layer species (e.g., shrubs, mosses (genus only), herbs, grasses, and fungi) were made at 10 randomly selected points along two 50-m transects (for a total of 20 plot measurements at each site). Estimates were made using a 1-m^2 wooden frame that had nails placed along each side at 10-cm increments; strings were tied between the nails to form a flexible grid. Aerial vegetative coverage was determined by counting the number of grid squares occupied by a particular species. Species that did not cover an entire 10 $\times$10-cm square were assigned a value of 1% to indicate their presence on the plot. Due to the overlapping layers of shrub and moss species, the sum of all percent cover estimates could equal more than 100% for a given plot. Statistical analysis of data was based upon the mean percent cover for each species reported within a given stand.

4. Results

4.1. Soil Temperature

[13] In all burn–control pairs, soil temperatures in burned stands exceeded those in the control throughout the entire growing season. The effect of fire on soil temperature was most pronounced in the 1990 burn where mean temperatures in the burned stand were 5.8°C (10 cm) to 6.6°C (20 cm) warmer than in the control. Averaged over the entire growing season, mean soil temperature at 20 cm below the forest floor surface increased by a factor of 4 to a maximum value in the first 3 years after fire and then declined steadily at a rate of 0.09°C yr^{-1} (Figure 2). The absence of a measurable temperature response in the 1-year-old stand can be at least partly attributed to the relatively low severity of that particular fire, which left between 25 and 30 cm of organic material on the surface. However, several studies have noted that fire effects may take several years to substantially influence soil temperature [*Burke et al.*, 1997]. As mosses and other understory plants reestablish themselves, the amount of organic matter on the surface increases and soil temperatures decline to preburn levels.

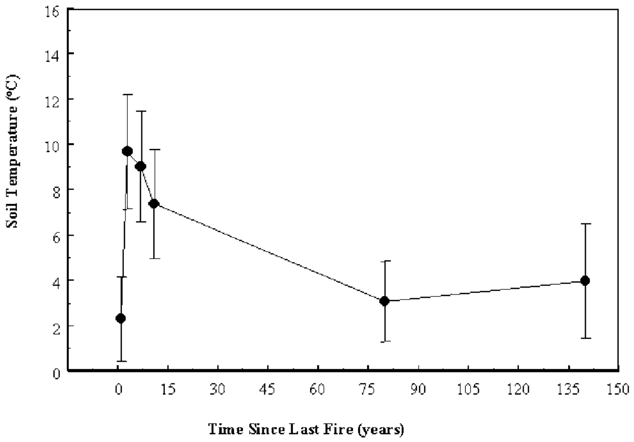

Figure 2. Mean seasonal temperature at 20 cm below the surface of the forest floor in a chronosequence of burned black spruce stands. Symbols represent the mean ± 1 s.d. of all measurements collected at that stand from May to August 1997 (n = 120).

4.2. Seasonal and Decadal Patterns of Soil CO_2 Efflux

[14] With the exception of the 1990 burn, mean respiration rates in burned stands were 50–60% of those observed in controls throughout the entire growing season (Figure 3). In general, peak rates of respiration occurred during late July and early August when air and soil temperatures reached their maximum values. The 1994, 1990, and 1987 burns all experienced a sharp peak in respiration during the third week of July (Julian days 208 and 209) that corresponded to record high levels of precipitation in 1997 in which more than 45% of mean annual precipitation (10.9 cm) occurred over a 2-week period National Weather Service, Alaska region (data available at http://www.wrcc.dri.edu/summary/climsmak.htm, 2000). Second-order polynomial regression models fit through the data were significant for the 1990 and 1996 burn but not for the 1994 and 1987 sites.

[15] Mean soil respiration increased as a function of stand age from 0.34 ± $0.17_{s.d.}$ g CO_2 m^{-2} hr^{-1} in the first year after fire to 0.92 ± $0.37_{s.d.}$ g CO_2 m^{-2} hr^{-1} in the 140-year-old stand. The average rate of increase along the chronosequence was 0.005 g CO_2 m^{-2} hr^{-1} yr^{-1} (0.12 Mg C ha^{-1} yr^{-2}). A logarithmic regression model provided the best fit to the seasonal mean respiration at each site and explained

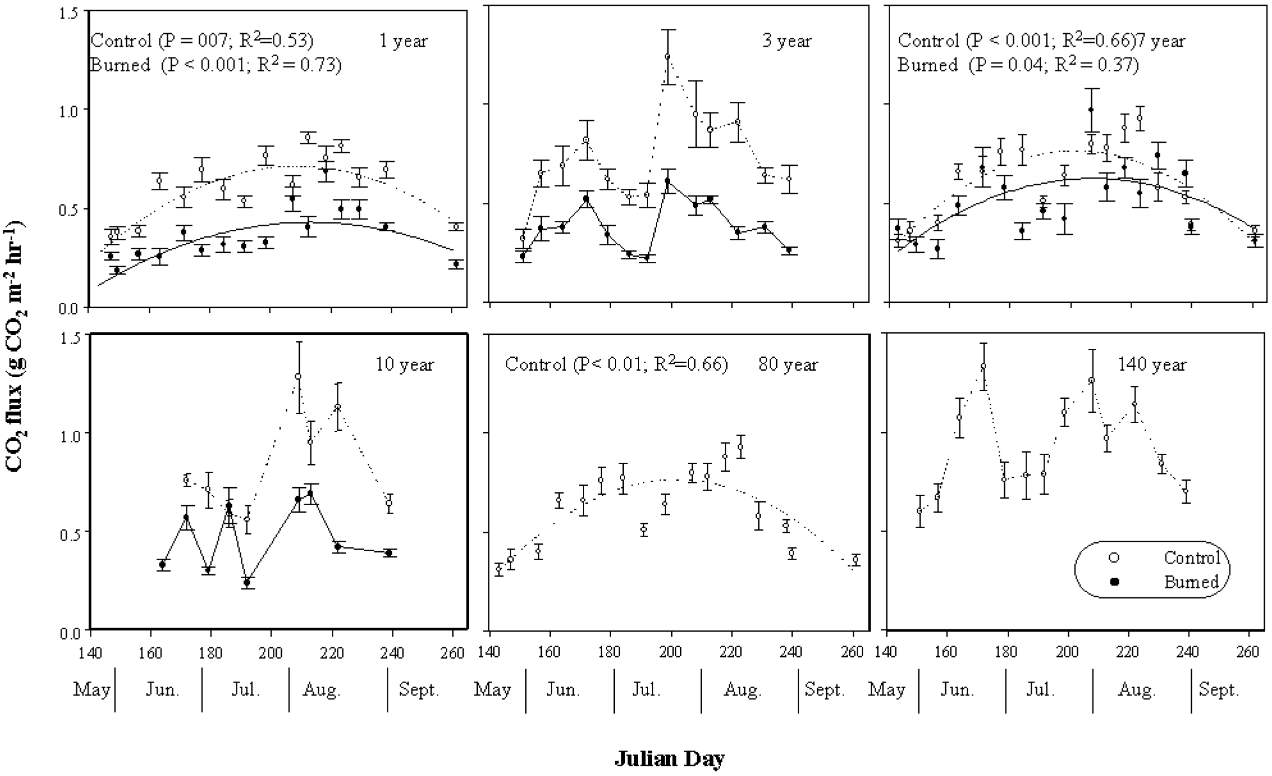

Figure 3. Seasonal patterns of CO_2 efflux in burned and control black spruce stands (May–August 1997). Symbols represent the mean ± 1 s.d. of 10 measurements. Closed symbols indicate data from burned stands; open symbols represent data from control stands. Data were fit with second-order polynomial regression models using sampling date as the independent variable and the mean of the 10 replicate samples collected within the stand at each time period as the dependent variable (n = the number of sampling dates). Regression curves are only shown where $P \leq 0.05$. Note that the control for the 7-year-old stand is also used as the 80-year-old stand in the chronosequence.

75% of the variation in the data (Figure 4a). A similar pattern was also observed in a smaller set of data collected in July 1996 in which soil respiration increased from $0.36 \pm 0.18_{\mathrm{s.d.}}$ to $1.51 \pm 0.49_{\mathrm{s.d.}}$ g CO_2 m^{-2} hr^{-1} across the 140-year chronosequence; the mean rate of increase was 0.008 g CO_2 m^{-2} hr^{-1} yr^{-1} (0.19 Mg C ha^{-1} yr^{-2}). Due to the restricted sampling schedule in 1996, a comparison between respiration rates in both years is limited to samples collected during the month of July (Figure 4b). Although differences in mean respiration rate at the two most recent burns (1996 and 1994) were not statistically significant, at all other burned sites, emissions in 1996 were significantly higher than those collected in 1997 ($P < 0.05$). Averaged across all stands, mean CO_2 efflux in 1996 was 45% higher in burned stands and 21% higher in control stands compared with 1997.

[16] Large differences in seasonal CO_2 emissions emphasize the potential magnitude of interannual variability in black spruce systems. Due to the high correlation between soil temperature and CO_2 emissions from root and decomposition [*Singh and Gupta*, 1977; *Van Cleve et al.*, 1981; *Tryon and Chapin*, 1983; *Schlentner and Van Cleve*, 1985; *Bonan and Van Cleve*, 1991], variation in seasonal climatic patterns and the depth of thaw has a large effect on the magnitude of CO_2 efflux during the growing season. It is also likely that a portion of this variability is the result of differences in sampling strategies between the 2 years. In 1997, a set number of samples were collected on a weekly basis whereas in 1996 the emphasis was on intensive measurements at a single site throughout an entire day. As a result, measurements at a given fire site were collected on fewer dates and sampling dates were not evenly distributed throughout the month. The most rigorous comparison of year-to-year variability is the 1990 fire site, which was sampled intensively in both years. Interannual variation in this site was even greater that suggested by the treatment means, with CO_2 efflux rates from 29% and 59% greater in 1996 for control and burned stands, respectively, compared with 1997.

4.3. Changes in Understory Vegetation

[17] One year after burning, $96.5 \pm 1.7_{\mathrm{s.e.}}$ % of the ground surface was either bare or covered with char (Table 2). No mosses had colonized the site and understory vegetation was dominated by *E. pratens* (meadow horsetail) and *R. acicularis* (prickly rose). Percent cover of understory species (mosses, shrubs, herbs, and grasses) increased from $9.8 \pm 10.8_{\mathrm{s.e.}}$ % in the 1-year-old stand to $153.2 \pm 27.4_{\mathrm{s.e.}}$ % in the 140-year-old stand. Rates of recovery of total vegetation cover were most rapid in the early part of the chronosequence, with more than half of the increase (57.7%) occurring in the first 10 years. A logarithmic regression of mean

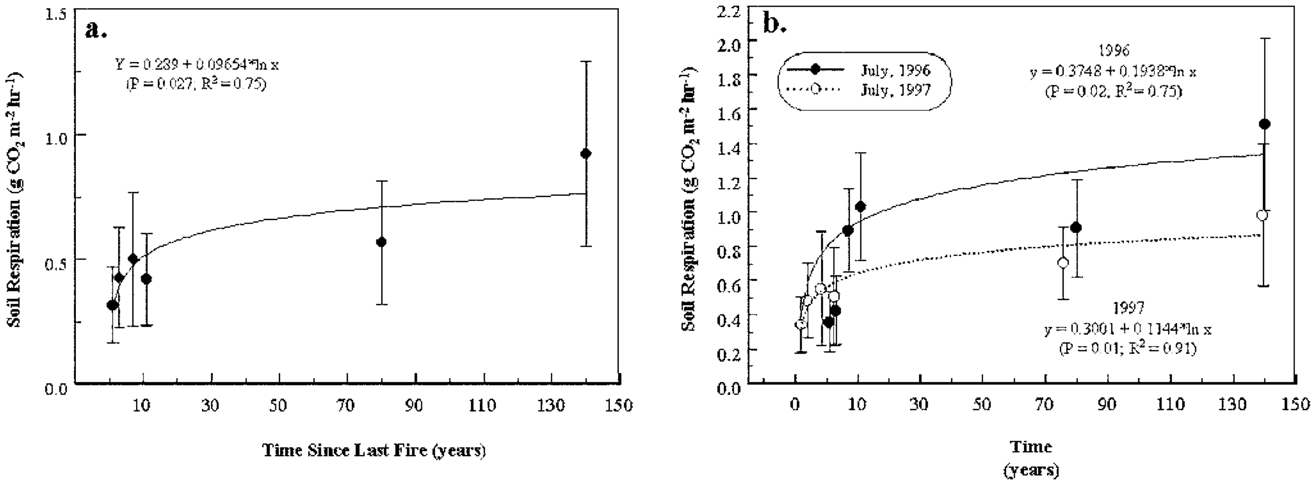

Figure 4. (a) CO_2 efflux as a function of time since last fire. Symbols represent the mean ± 1 s.d. of all measurements collected within a chronosequence stand from May to September 1997. For the 1 and 7 year old stands, n = 160, for the 3 and 140 year old stands, n = 130, and for the 11-year-old stand, n = 80. Data were fit with a logarithmic regression model through the mean value (n = 6). (b) Comparison of CO_2 efflux as a function of time since last fire in July 1996 and 1997. Symbols represent the mean ± 1 s.d. of all measurements collected within a chronosequence stand during the month of July. Data were fit with a logarithmic regression model through the mean values for each stand age (n = 6).

percent cover (shrubs, herbs, grasses, and mosses) against stand age was highly significant and yielded an R^2 of 0.87 ($P = 0.002$).

[18] The pattern of increasing soil CO_2 efflux as a function of increasing stand age exhibited in both the 1996 and 1997 data is consistent with the rapid reestablishment of understory biomass and mosses during the first decade after fire. An exponential regression of mean seasonal soil respiration in 1997 on percent ground cover of understory species (mosses, shrubs, grasses, and herbs) yielded an R^2 of 0.89 ($P = 0.008$) (Figure 5). This suggests that increases in root and moss biomass in the decades following fire may be one of the primary regulators of total soil CO_2 efflux.

4.4. Carbon and Nitrogen Storage in Organic Soil Horizons

[19] Carbon and nitrogen storage in organic horizons were estimated from the product of mean carbon concentration and mean organic soil bulk density following:

$$\mathrm{SES} = \Sigma(\mathrm{E})(\mathrm{BD})(\mathrm{T_h}) \qquad (1)$$

where SES represents soil carbon or nitrogen storage, E is carbon or nitrogen concentration (weight %), BD is bulk density (g cm^{-3}), T_h is the soil layer thickness (cm), and the summation is over all organic soil layers [*Marion and Oechel*, 1993]. Due to the limited amount of moss regrowth in recently burned stands, we were unable to collect volumetric samples for determination of bulk density in the moss horizon. Data from the 3, 7, and 10 year old stands were aggregated together and the mean value used to estimate carbon and nitrogen density for "burned" stands (such that n = the number of core samples). Similarly, data from four unburned stands were aggregated to provide mean values for "unburned" stands. Due to the random location of core samples, not all samples contained the same genetic horizons. For this reason, the number of samples for a given horizon does not necessarily equal 40.

[20] For unburned soils, mean concentrations of carbon and nitrogen in moss, fibric, and humic horizons were not significantly different (Table 3). However, both burned and control samples did exhibit a significant increase in bulk density with depth. In the unburned samples, mean bulk densities in moss and humic materials differed by an order of magnitude, reflecting the greater degree of consolidation in more highly decomposed materials. This difference was even more pronounced in the burned soils, with an increase in bulk density between fibric and humic horizons of more than 200%. Significant differences also existed between the same organic horizons in burned and control stands. The bulk densities of fibric and humic soils in the burned stand (0.15 ± 0.08 and $0.48 \pm 0.18_{\mathrm{s.d.}}$ g cm^{-3}, respectively) were approximately twice as high as those of the control stands (0.08 ± 0.05 and $0.21 \pm 0.09_{\mathrm{s.d.}}$ g cm^{-3}), perhaps reflecting the consolidation of materials following combustion. As a result of these differences in bulk density, the mean carbon and nitrogen densities (SES) of burned organic materials (fibric and humic) were 1.5–2.5 times greater than those from control stands.

4.5. Rates of Carbon and Nitrogen Accumulation Following Fire

[21] Rates of postfire carbon and nitrogen accumulation were determined by plotting SES as a function of stand age (Figures 6a and 6b). C and N densities from burned stands were used to estimate carbon and nitrogen storage at the 3, 7, 11, and 41 year old sites and the unburned carbon density values were used to estimate carbon storage in older stands (Figure 6a). Carbon storage in the organic profile (moss, fibric, and humic horizons) increased from $89.2 \pm 34.7_{\mathrm{s.d.}}$ Mg ha^{-1} in the 3-year-old stand to $157.7 \pm 27.1_{\mathrm{s.d.}}$ Mg ha^{-1}

Table 2. Percent Cover of Understory Vegetation Along a Black Spruce Chronosequence

		Stand age (year of most recent fire)						
		1 (1996)	3 (1994)	7 (1990)	10 (1987)	41 (1956)	80 (1915)	140 (1855)
Shrubs	*A. uva–ursi*	–	–	–	–	–	–	0.4 ± 0.3 (15%)
	E. nigrum	–	–	–	–	0.1 ± 0.0 (5%)	5.4 ± 1.7 (55%)	1.5 ± 0.7 (30%)
	L. groenlandicum	–	1.3 ± 1.3 (10%)	0.5 ± 0.5 (5%)	2.3 ± 1.4 (15%)	28.0 ± 4.7 (100%)	4.1 ± 1.4 (45%)	14.6 ± 1.9 (100%)
	R. acicularis	1.2 ± 0.8 (15%)	0.2 ± 0.2 (5%)	3.8 ± 1.3 (35%)	8.5 ± 2.0 (90%)	0.3 ± 0.2 (15%)	0.4 ± 0.3 (15%)	0.3 ± 0.3 (10%)
	Salix spp.	–	3.6 ± 1.5 (50%)	20.4 ± 6.6 (50%)	1.5 ± 1.5 (5%)	17.6 ± 4.3 (90%)	9.9 ± 2.1 (80%)	2.0 ± 1.5 (10%)
	V. myrtilloides	–	–	–	–	20.3 ± 4.1 (95%)	–	2.1 ± 0.7 (45%)
	V. uliginosum	–	–	–	5.1 ± 3.3 (30%)	–	–	4.2 ± 1.7 (45%)
	V. vitis–idea	–	–	1.6 ± 0.9 (20%)	–	–	11.2 ± 2.2 (95%)	13.3 ± 2.1 (95%)
Bryophytes	*C. purpureus*	–	59.4 ± 6.4 (95%)	26.2 ± 5.9 (90%)	35.5 ± 5.5 (95%)	–	–	–
	H. revolutum	–	–	–	–	4.5 ± 1.3 (50%)	–	–
	H. splendens	–	–	–	–	1.6 ± 0.5 (40%)	57.5 ± 7.7 (95%)	54.5 ± 6.2 (100%)
	P. schreberi	–	–	–	–	15.8 ± 3.6 (95%)	4.0 ± 1.6 (45%)	11.8 ± 2.8 (65%)
	P. juniperinum	–	–	0.1 ± 0.1 (5%)	3.9 ± 0.9 (55%)	–	–	–
	Sphagnum spp.	–	–	–	–	–	3.8 ± 3.9 (5%)	6.2 ± 3.3 (30%)
Herbs	*E. angustifolium*	–	11.9 ± 1.5 (95%)	2.9 ± 0.8 (80%)	6.0 ± 0.8 (100%)	–	–	–
	F. virginiana	–	–	–	–	–	0.1 ± 0.1 (5%)	–
	G. lividum	–	–	–	–	–	–	0.4 ± 0.5 (40%)
	P. fruticosa	–	–	–	–	6.5 ± 2.6 (60%)	–	–
	R. chamaemorus	–	0.3 ± 0.0 (5%)	–	–	–	1.0 ± 2.1 (45%)	5.4 ± 1.8 (85%)
	Other	4.8 ± 1.7 (65%)	–	4.5 ± 2.0 (25%)	3.1 ± 0.7 (65%)	4.1 ± 1.4 (45%)	0.3 ± 0.7 (15%)	0.6 ± 0.8 (30%)
Lichens	*Cladonia spp.*	–	0.3 ± 0.0 (5%)	–	–	0.3 ± 0.1 (15%)	–	0.4 ± 0.1 (20%)
	C. rangiferina	0.3 ± 0.3 (5%)	–	–	–	–	4.0 ± 1.3 (55%)	3.5 ± 1.5 (50%)
	Peltigera spp.	–	12.0 ± 3.9 (55%)	0.5 ± 0.5 (5%)	–	2.9 ± 1.1 (40%)	8.2 ± 1.5 (75%)	7.2 ± 1.7 (80%)
Horsetails	*E. pratens*	3.9 ± 1.6 (35%)	17.8 ± 2.8 (100%)	1.5 ± 0.8 (15%)	2.5 ± 0.5 (70%)	1.6 ± 0.5 (65%)	0.4 ± 0.2 (15%)	21.4 ± 13.1 (95%)
Grasses	*Calamagrostis spp.*	0.1 ± 0.2 (5%)	0.9 ± 0.74 (10%)	8.5 ± 3.2 (15%)	21.4 ± 5.4 (100%)	10.2 ± 2.5 (80%)	6.5 ± 4.5 (30%)	5.2 ± 6.3 (75%)
Fungi		–	0.1 ± 0.1 (10%)	–	–	0.1 ± 0.0 (5%)	–	0.3 ± 0.5 (30%)
Ferns	*D. austriaca*	–		–	2.7 ± 1.1 (35%)	–	0.1 ± 0.1 (5%)	–
Other	Bare/Char	96.5 ± 1.7 (20%)	19.2 ± 3.1 (70%)	31.2 ± 6.5 (80%)	10.0 ± 3.2 (50%)	–	–	–
	Dried vegetation	–	7.5 ± 1.3 (90%)	4.3 ± 0.5 (25%)	30.5 ± 4.9 (100%)	5.9 ± 1.1 (14%)	4.1 ± 1.9 (35%)	1.6 ± 0.8 (10%)
	Litter	18.3 ± 7.4 (35%)	–	3.8 ± 2.3 (15%)	–	2.0 ± 1.6 (10%)	–	1.8 ± 0.5 (10%)
	Wood	8.9 ± 8.2 (70%)	18.9 ± 3.5 (90%)	3.7 ± 1.2 (45%)	13.8 ± 3.0 (90%)	5.0 ± 1.5 (40%)	3.8 ± 1.3 (55%)	1.5 ± 0.0 (5%)

Plant identification follows *Johnson et al.* [1995]. Values represent the mean ± 1 s.e. of 20 measurements at each site. Dashed lines indicate the absence of a species. The number in parentheses indicates the percentage of sample plots that contained individuals of that species.

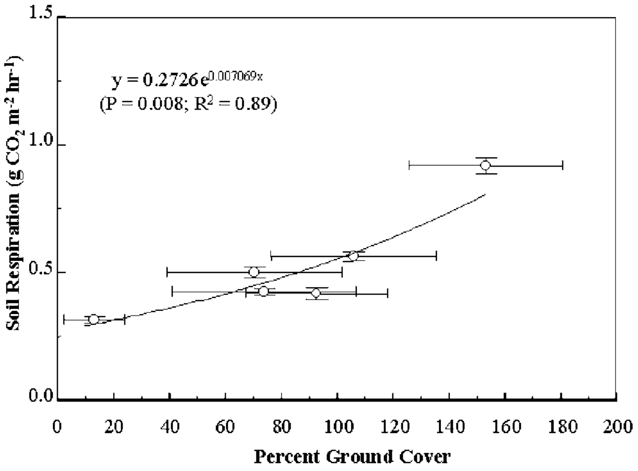

Figure 5. Mean soil CO_2 efflux as a function of percent cover of shrubs, mosses, herbs, and grasses. Symbols represent the mean of all measurements collected at a stand from May to August 1997. Vertical error bars indicate ± 1 s.e. of CO_2 flux; horizontal error bars indicate ± 1 s.e. of percent cover estimates made at 20 sampling points per stand (n = 20). Data were fit with an exponential regression model through the mean values (n = 6).

in the 140-year-old stand. The rate of increase along the chronosequence was linear ($P = 0.002$; $R^2 = 0.92$), with a mean carbon accumulation rate of 0.54 Mg C ha^{-1} yr^{-1}. Based on the slope of the accumulation curve, it appears that carbon storage in organic horizons had yet to reach steady state 140 years after the fire.

[22] Due to potential differences in fire severity in chronosequence stands, accumulation rates calculated using the entire thickness of the organic profile represent maximum estimates. Within each fire scar, some fraction of the preburn humic horizon was not combusted and cannot be attributed to reaccumulation during this fire cycle. In addition, division of this horizon into preburn and postburn carbon was hampered by the lack of discrete charcoal layers or other markers within the humic profile. For this reason, a more conservative estimate for carbon accumulation should include only that carbon that was added to the moss and fibric horizons (i.e., the "shallow" carbon pool of *Goulden et al.* [1998] and *Harden et al.* [1997, 2000]). Carbon accumulation under this more conservative estimation is also linear over the entire age sequence ($P = 0.006$; $R^2 = 0.88$). However, the mean rate of carbon accumulation is reduced to 0.28 Mg C ha^{-1} yr^{-1}.

[23] As with carbon accumulation, rates of nitrogen accumulation were determined for both maximum (total organic profile) and minimum (moss and fibric horizons) scenarios (Table 3). Total profile nitrogen content did not appreciably increase with stand age in the chronosequence sites (Figure 6b). This may be attributed to the large variability in nitrogen storage in the humic horizon as well as to relatively low rates of nitrogen inputs to the system. However, nitrogen content in the moss and fibric horizons (minimum N accumulation scenario) did show a linear increase over the 140-year chronosequence ($P = 0.006$; $R^2 = 0.87$) with a mean accumulation rate of 0.0076 Mg N ha^{-1} yr^{-1}. These accumulation rates are on the same order of magnitude as annual nitrogen uptake reported for black spruce forests near Fairbanks (0.003–0.01 Mg N ha^{-1} yr^{-1}) [*Van Cleve et al.*, 1983]. Despite the great variability in nitrogen storage in the total organic profile, the percentage of nitrogen contained in the humic horizon steadily decreased with increasing stand age, from 91.4% in the 3-year-old stand to 61.3% in the 140-year-old stand.

[24] A number of studies in moss-derived soils have shown a strong vertical gradation in carbon and nitrogen concentration due to increasing decomposition as a function of depth in the profile [*Harden et al.*, 1997; *O'Neill et al.*, 1995; *Veldhuis and Knapp*, 1998]. The absence of a similar pattern in Table 3 is most likely a result of difficulties in subdividing the samples into genetic horizons while in the field. Due to the apical growth form of many boreal moss species, new growth is added to the end of the stem while older material decomposes in place. As such, the boundary between living, nonphotosynthetic tissue and slightly decomposed fibric material is not distinct and may be difficult determine in the field. Incorporation of even a small amount of fibric material into a moss sample would lower the mean carbon concentration without significantly altering its bulk density. The importance of these potential sampling errors is minimized by constraining our estimates of carbon accu-

Table 3. Bulk Density, Carbon, and Nitrogen Contents for Organic Horizons of Burned and Unburned Black Spruce Soils

	% Carbon	% Nitrogen	Density (g cm^{-3})	C Density (Mg ha^{-1})	N Density (Mg ha^{-1})
			Unburned		
Moss	35.29 ± 10.09 (31) a	0.98 ± 0.67 (31) a	0.0329 ± 0.014 (43) a	1.16 ± 0.33	0.032 ± 0.022
Fibric	35.18 ± 8.77 (33) a	0.96 ± 0.42 (33) a	0.0793 ± 0.054 (58) b	2.78 ± 0.72	0.076 ± 0.034
Humic	33.00 ± 7.60 (17) a	0.81 ± 0.33 (17) a	0.205 ± 0.088 (26) c	6.77 ± 1.58	0.166 ± 0.068
			Burned		
Moss	38.27 ± 2.28 (9) a	1.28 ± 0.23 (9) b	–	–	–
Char/Fibric	35.78 ± 8.31 (41) a	0.99 ± 0.36 (41) a	0.147 ± 0.08 (53) d	5.26 ± 1.25	0.146 ± 0.054
Humic	21.54 ± 8.54 (30) b	0.89 ± 0.34 (30) a	0.483 ± 0.18 (41) e	10.40 ± 4.14	0.430 ± 0.164

Values represent the mean ± 1 s.e.; the number of samples is provided in parentheses. Carbon and nitrogen densities were determined as the product of mean %C or %N, and mean density. Variance was determined from the product of variance equation presented by *Schumacher and Chapman* [1954]. Differences between mean values were determined by paired t-tests. Within each column, items marked by the same letter are not significantly different ($\alpha = 0.05$).

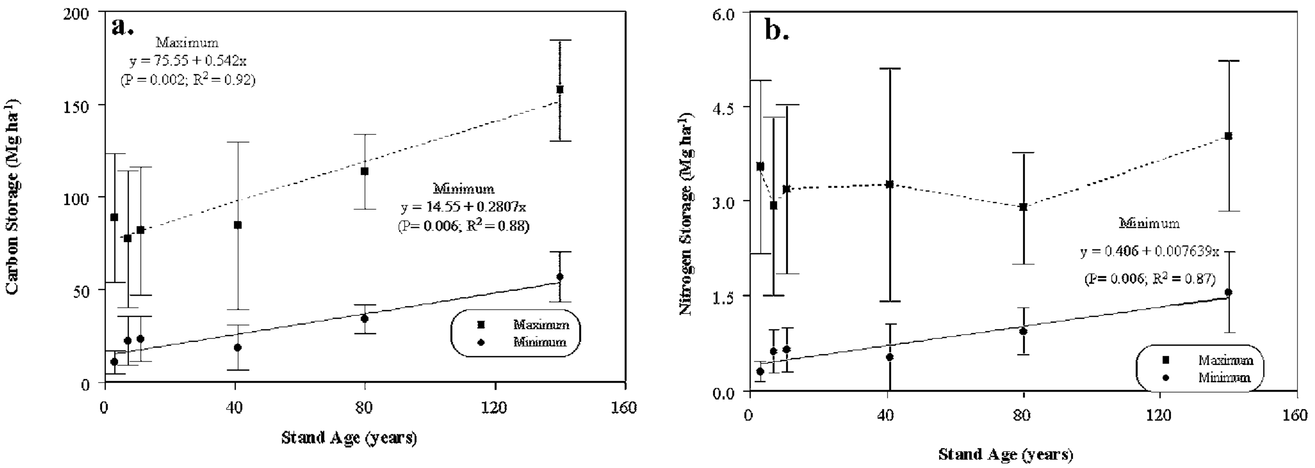

Figure 6. (a) Maximum (total organic profile) and minimum (moss and fibric horizons) scenarios for carbon accumulation in the organic profile in a chronosequence of burned black spruce stands. Symbols represent mean ± 1 s.d. Data were fit with a linear regression model through the mean value for each stand age (n = 6). Variance was determined as in Table 3. (b) Maximum (total organic profile) and minimum (moss and fibric horizons) scenarios for nitrogen accumulation in the organic profile in a chronosequence of burned black spruce stands. Symbols represent mean ± 1 s.d. Data were fit with a linear regression model through the mean value for each stand age (n = 6). Variance was determined as in Table 3.

mulation rates between a minimum (moss and fibric only) and maximum (whole profile) value. Despite these limitations, rates of carbon and nitrogen accumulation measured in the chronosequence approach agree favorably with values reported in the literature (Table 4).

5. Discussion

[25] Determination of postfire carbon exchange is complicated by the fact that CO_2 production has several sources, and is the net result of many distinct microbial and metabolic processes [*Schimel and Gulledge*, 1998]. In boreal soils, CO_2 flux from the forest floor (F_c) represents the net result of microbial decomposition, root and moss respiration, and photosynthetic uptake by surface mosses:

$$F_c = (M_R - M_P) + A_R + H_R \qquad (2)$$

where M_R is moss respiration, M_P is moss photosynthesis, A_R is autotrophic respiration (roots), and H_R is heterotrophic respiration (decomposition). Each of these processes is affected differently by fire and, thus, the proportion of soil respiration contributed by each component may be expected to change as a soil recovers from disturbance.

[26] In recently burned stands, contributions from mosses and roots are greatly reduced or absent (M_R, M_P,and $A_R \approx 0$), resulting in reduced rates of F_c relative to unburned controls throughout the growing season (Figure 3). As trees, understory vegetation, and mosses begin to reestablish themselves, respiratory activity in roots and mosses increases, resulting in increased levels of total soil CO_2 flux as a function of stand age (Figures 4a, 4b and 5). All of the components of soil CO_2 flux are sensitive to changes in environmental variables such as soil temperature and moisture. This generalized environmental response can be observed both in the parabolic patterns of seasonal CO_2 flux that parallel changes in air and soil temperature during the growing season and in the sharp increase in respiration in response to record high levels of precipitation in late July (National Weather Service, Alaska region, data available at http://www.wrcc.dri.edu/summary/climsmak.htm, 2000). Soil moisture also appears to play a significant role in regulating seasonal patterns of CO_2 exchange, as evidenced by the pattern of declining CO_2 emissions during a period of midsummer drying (early July) followed by a sharp increase in activity following record levels of precipitation in late July (Figure 3).

Table 4. Comparison of Input, Decomposition, and Carbon Accumulation Terms to Values Reported in the Literature

	Input (Mg C ha^{-1} yr^{-1})	Decomposition (yr^{-1})	C accumulation (Mg ha^{-1} yr^{-1})
Trumbore and Harden [1997]	0.3–0.9	0.004–0.018	–
	0.5–1.5	0.004–0.028	–
Harden et al. [1997]	–	–	0.2–0.4
Trettin et al. [1995]	0.7–5.4	–	0.1–0.8
Schlesinger [1990]	–	–	0.008–0.12
Tolonen et al. [1992]	–	–	0.08–0.41
This study			
Microbial incubations	–	0.002–0.017	
Numerical model	1.833	0.002	
Chronosequence			0.28–0.54

[27] Although the pattern of increasing F_c over decadal timescales appears to be strongly linked to the reestablishment of shrub and herb species (Figure 5), postfire changes in soil temperature, moisture, and substrate quality undoubtedly also play an important role in regulating rates of carbon exchange. Following fire, the soil surface is darkened and shading from the forest canopy is eliminated, providing a greater input of heat energy to the soil surface. At the same time, trees, mosses, and organic horizons are partially to completely removed, reducing heat losses to the atmosphere through evapotranspiration and allowing for greater penetration of heat into the soil profile. Over time, these changes result in increased soil temperatures (Figure 2), deepening of the permafrost active layer, and enhanced soil drainage [*Viereck*, 1975, 1982; *Wein and Bliss*, 1973; *Wein*, 1976; *Tarnocai and Zoltai*, 1978; *Dyrness*, 1982; *Mackay*, 1995; *Swanson*, 1996; *O'Neill*, 2000]. In addition, deposition of ash minerals following fire decreases soil acidity and introduces a pulse of nutrients into the upper portion of the soil profile. Given the extreme temperature and nutrient limitations of these systems, these changes in the soil environment have the potential to dramatically increase rates of decomposition in the months and years following disturbance [*Richter et al.*, 2000; *O'Neill*, 2000]. However, due to the low rates of decomposition typical of black spruce systems [*Flanagan and Van Cleve*, 1977] even large increases in decomposition may easily be masked by relatively smaller changes in root respiration.

[28] Although there is convincing evidence to support the hypothesis that changes in the soil environment (e.g., temperature, moisture, and nutrient status) result in enhanced rates of decomposition [*Richter et al.*, 2000; *Goulden et al.*, 1998; *Burke et al.*, 1997; *Bonan and Van Cleve*, 1991; *Van Cleve and Yarie*, 1986; *Schlentner and Van Cleve*, 1985; *Flanagan and Van Cleve*, 1977], neither the magnitude nor the duration of this source has been adequately quantified. However, it has been estimated that postfire releases of carbon may equal of exceed the amount of CO_2 released during combustion itself [*Auclair and Carter*, 1993; *Richter et al.*, 2000]. Since these postfire microbial emissions are not balanced by an equivalent uptake of carbon in vegetation this represents a net loss of stored carbon to the atmosphere. However, determining the ecological significance of these postfire carbon losses requires a detailed understanding of the balance between short-term losses of carbon during and immediately after combustion and the gains of carbon in tree and moss biomass during forest regrowth. In order to examine these temporal patterns in greater detail, we combined our field measurements with a mass balance model of decomposition, carbon inputs, and carbon accumulation.

5.1. Patterns of Carbon Input and Decomposition Rates Following Fire: A Mass Balance Model

[29] The carbon balance of an ecosystem is the difference between carbon uptake as CO_2 during photosynthesis and the respiratory loss of carbon as CO_2 by plants, animals, and de-composer organisms. For this reason, the soil carbon accumulation curve (Figure 6a) contains information about the temporal pattern of carbon inputs and losses during soil development. In general, the accumulation of carbon in a newly developing soil follows a logarithmic pattern with an initial period of rapid carbon accumulation that declines slowly over time until the system reaches an equilibrium level of carbon storage. This relationship may be represented as:

$$dC/dt = I - kC \tag{3}$$

or, in an integrated form

$$C_t = I/k\left(1 - e^{-kt}\right) \tag{4}$$

where C is carbon storage, I is carbon input to the soil system through net primary productivity (NPP), and k is a first-order decomposition coefficient [*Jenny et al.*, 1949; *Olson*, 1962; *Harden et al.*, 1992, 1997].

[30] Several studies of boreal carbon sequestration have used a mass balance approach to estimate long-term rates of NPP and decomposition by fitting equation (4) to a carbon accumulation curve (C_t) and solving for I and k [*Harden et al.*, 1992, 1997; *Rapalee et al.*, 1998; *Trumbore and Harden*, 1997]. Although this approach has successfully predicted input and decomposition constants over millennial timescales, the steady state model requires several assumptions that may limit its utility in modeling postfire carbon accumulation over shorter timescales (<100 years): (1) mathematically, the model requires carbon storage at time 0 to be equal to zero and (2) rates of decomposition and inputs are constant. Both of these assumptions are violated in fire-dominated northern ecosystems.

[31] *Harden et al.* [2000] addressed these concerns by partitioning the soil carbon component into three functional pools that each had different inputs, turnover times, and responses to fire disturbance. However, for this study, we did not have all of the information needed to parameterize the *Harden et al.* [2000] model and instead approached the problem numerically. Long-term input and decomposition terms were simulated using a model of carbon accumulation that was based on equations (3) and (4) but allowed both decomposition and NPP to vary over the fire cycle. Postfire decomposition was modeled as a decreasing exponential function of the form:

$$k(t) = k' + be^{-ct} \tag{5}$$

where k' is the long-term mean decomposition rate, b is the maximum rate of decomposition following fire, c is the slope of the exponential function, and t is time (years). The use of an exponential decomposition function is justified by the pattern of elevated soil temperatures observed in the first years after fire (Figure 2) and the strong correlation between soil temperature and microbial activity noted in a number of studies of boreal and temperate soils [e.g., *Flanagan and Veum*, 1974; *Singh and Gupta*, 1977; *Bunnell et al.*, 1977; *Schlentner and Van Cleve*, 1985]. In addition, microbial incubation experiments on recently burned and control black spruce soils from this same region of the Alaskan interior suggested that changes in substrate chemistry further enhanced rates of decomposition in the first years after fire, and that the effect of these substrate changes declined as the stand recovered from disturbance [*O'Neill*, 2000].

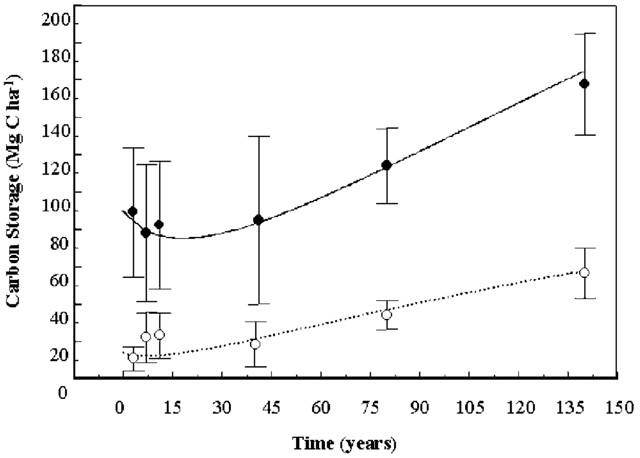

Figure 7. Comparison of modeled carbon accumulation with field data for minimum and maximum carbon storage scenarios. Symbols represent the mean ± 1 s.d. of field data. Lines represent simulated carbon accumulation rate from numerical model.

[32] Inputs to the systems were approximated by an exponential equation of the form:

$$I(t) = M + D[\ln(at)] \qquad (6)$$

where M, a, and D are constants of integration defining the position of the curve relative to the origin, the rate of increase, and the inflection point for the curve. Although this model may overestimate inputs in the first decade after fire, use of the exponential function is supported by the pattern of increasing ground cover after fire and provides a more conservative estimation of the postfire carbon source. In order to reduce the complexity of the model, we first imposed the following boundary conditions:

$$k(0) = k_{\max} \qquad (7)$$

$$k(\infty) = k' \qquad (8)$$

$$I(\infty) = I' \qquad (9)$$

where $k_{\max}$ is the maximum rate of decomposition that occurs after a fire and I' is the long-term steady state rate of NPP. These assumptions imply that as the time since fire becomes very large, both k and carbon inputs approach their long-term mean values. For this reason, initial values for k' and M may be approximated by fitting the steady state model (equation (4)) to a carbon accumulation curve and solving for the input and decomposition parameters. The model was initialized using steady state values for M and k' and the remaining variables were allowed to vary during multiple iterations until the best fit to the data in Figure 6a was obtained (Figure 7). The model was run for both the maximum and minimum carbon accumulation scenarios.

5.2. Model Results

[33] In the maximum accumulation scenario, decomposition after fire increased by a factor of 3.5 from a long-term average of 0.006 yr^{-1} to a maximum value $(b + k')$ of 0.021 yr^{-1} (Table 5). Elevated decomposition rates (more than 5% above the long-term average) persisted for the first 49 years after fire. During the first 100 years after fire, carbon inputs to the soil system increased from 0.0 to 1.5 Mg ha^{-1}; more than half of this increase occurred during the first decade. In the minimum carbon accumulation scenario, both long-term rates of decomposition (0.008 yr^{-1}) and the increase in decomposition after fire (0.31 yr^{-1}) were greater than in the maximum case scenario. However, the timescale of enhanced decomposition was approximately the same (54 years). Carbon inputs were about half (48%) those in the maximum scenario, reaching a value of 0.75 Mg C ha^{-1} by the end of the first 100 years after fire. For both maximum and minimum scenarios, decomposition and input parameters are well within the range of values determined from ^{14}C dating, mass balance approaches, chronosequence studies, and laboratory incubations (Table 4). In addition, the patterns of decreasing carbon storage in the first decade after fire are consistent with the prediction of theoretical models [e.g., *Bonan*, 1992; *Kasischke et al.*, 1995].

5.3. Source–Sink Potential of Boreal Forest Soils

[34] In order to determine the potential of burned soils to act as a net source of carbon, carbon inputs and decomposition derived from the model were plotted together as a function of time. The point where the two curves cross (C_P) represents the time at which inputs to and losses from the system are balanced. At time < C_P, decomposition exceeds inputs and there is a net loss of carbon from the ecosystem. Conversely, at time > C_P, inputs exceed decomposition and the system is a net sink for carbon. The difference between these two curves represents the net soil carbon balance.

[35] The model suggests that C_P occurs 7–14.5 years (minimum and maximum carbon accumulation scenarios, respectively) after burning (Figure 8). In the maximum scenario, the model suggests a net release of 11.0 Mg C ha^{-1} in the first 15 years after fire followed by a net accumulation of 78.4 Mg C ha^{-1} in the next 125 years (0.63 Mg C ha^{-1} yr^{-1}). In the minimum scenario, 1.8 Mg C ha^{-1} is released in the first 7.5 years after fire, followed by a

Table 5. Equations and Parameters Used in Numerical Model of Carbon Accumulation

Stocks:
Carbon storage (t) = Carbon storage (t − dt) + (Inputs − Decomposition * dt)
Inflows:
Inputs = a * ln(M * Time)
Outflows:
Decomposition = Carbon storage * k
Modifiers:
$k = k' + be^{-ct}$
Parameters:

	Maximum	Minimum
C storage (initial)	90	14
k′	0.006	0.008
b	0.015	0.03
c	0.08	0.08
M	0.9	1.2
a	0.33	0.15

Input parameter values were determined by regression of steady state carbon accumulation on field data. Optimal parameter values were then determined by iterative sensitivity analyses.

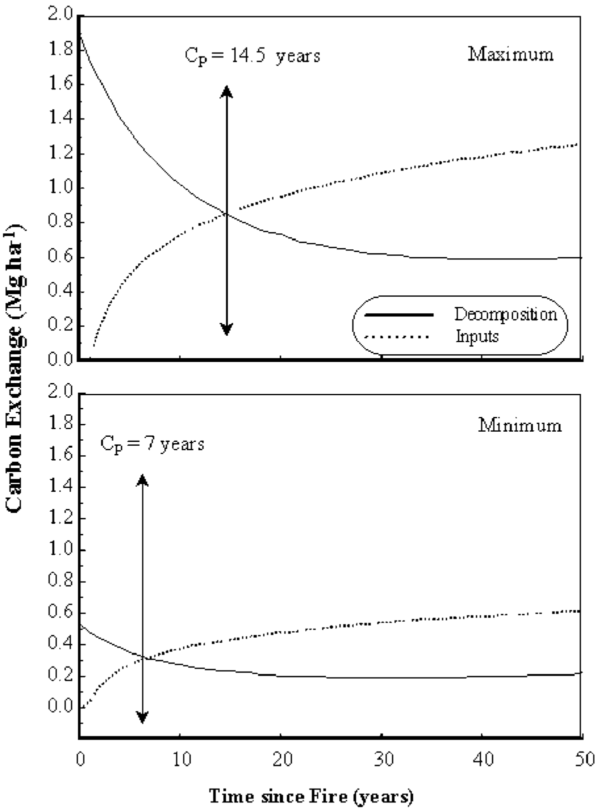

Figure 8. Modeled source–sink dynamics of black spruce soils following fire. Lines represent input and decomposition terms simulated using a steady state carbon accumulation model.

net accumulation of 45.7 Mg C ha^{-1} in the remaining 133 years (0.34 Mg C ha^{-1} yr^{-1}). Using the carbon densities in Table 3, these carbon losses suggest that 12.4–12.6% of organic profile carbon is released to the atmosphere following fire (maximum and minimum carbon accumulation scenarios, respectively).

5.4. Field and Model Limitations

[36] One limitation with the numerical modeling ap-proach presented in this paper is that the STELLA language does not allow for curve optimization. Best fits to the field data could only be determined by iterative sensitivity analyses. Because of this, we were not able to provide confidence intervals for curve fits. Where possible, the model was constrained by field and laboratory data. For example, decomposition coefficients were only allowed to vary within the range of values determined during laboratory incubation analyses [*O'Neill*, 2000] and the shape of the carbon input curve was based on ground cover data. In addition, because the model does not provide an analytical solution for the system, it was not possible to quantify the degree of fit statistically. Despite these quantitative limitations, the close agreement of model results with experimental data from this and other studies (Table 4) indicates that, as a first-order approximation, a mass balance approach can be useful in defining descriptive patterns of postfire carbon dynamics and may offer an alternative method for estimating decomposition and input coefficients in disturbed landscapes.

[37] In addition to statistical limitations within the model itself, interpretation of postfire accumulation rates is hampered by the low number of chronosequence points between 10 and 80 years of stand development. Model dynamics are highly sensitive to carbon storage in the 41-year-old stand. Location of additional chronosequence sites near major curve inflection points may greatly improve the accuracy of the model. Furthermore, the respiration and accumulation models described in this chapter only evaluate carbon dynamics in the organic horizons. As such, they likely underestimate true postfire losses from the soil. Warming of the mineral soil profile and deepening of the active layer have the potential to stimulate decomposition of carbon previously immobilized in permafrost [*O'Neill*, 2000; *Goulden et al.*, 1998; *Winston et al.*, 1997]. For this reason, it is possible for soils to be accumulating carbon in surface horizons while still functioning as a net source of carbon. In addition, recent modeling studies by Zhuang et al. (Modeling the soil thermal and carbon dynamics of a fire chronosequence in interior Alaska, in review) indicate that seasonal variability in climate plays a significant role in regulating carbon dynamics over decade to century timescales. The models described in this paper do not take into account the effects of seasonal climate variability.

[38] An additional limitation of the chronosequence design is intrasite variability arising from differences in fire severity in the differently aged stands. The response of soil and vegetation to burning depends to a large extent on the amount of organic matter removed by combustion [*Kasischke et al.*, 2000b]. A severe fire, or one that burns through the entire organic layer and leaves mineral soil exposed at the surface, will warm the soil to a greater extent and create different seedbed conditions than a fire in which only a portion of the organic mat is removed [*Kasischke et al.*, 2000b]. Although the effect of fire severity on reaccumulation of carbon and nitrogen in the soil profile was partially constrained by the use of maximum and minimum accumulation scenarios, differences in fire severity still need to be considered when interpreting chronosequence data. In particular, the relatively low severity of the 1-year-old site may result in an underestimation of both soil CO_2 recovery curves and carbon and nitrogen reaccumulation rates.

5.5. Implications for Carbon Storage Under Altered Fire Regimes

[39] The current generation of general circulation models predicts increases in both surface temperature and the frequency of drought in boreal regions. Under these conditions, both the frequency and severity of wildfires may be expected to increase [*Whalen*, 1995; *Wotton and Flannigan*, 1993; *Stocks et al.*, 2000]. Although the effects of these changes in the fire regime are uncertain, the numerical modeling approach presented above offers some insight into possible changes in carbon dynamics that might result from a decrease in the length of the fire cycle.

[40] In the absence of fire disturbance, total decomposition of carbon continues to increase until the system reaches a steady state; that is, annual inputs from NPP equal carbon losses through decomposition. Since decom-

Table 6. Simulated Effects of Changes in Fire Frequency on Carbon Storage in Organic Profiles

Length of fire cycle (years)	Carbon losses (Mg ha^{-1})	Carbon storage (Mg ha^{-1})	Net (Mg ha^{-1})	Percent decrease in C storage per one category increase in fire frequency
50	1.8–11.0	13.1–16.3	5.3–11.3	72.0–82.7%
100	1.8–11.0	32.4–51.3	30.6–40.3	48.9–61.0%
200	1.8–11.0	61.7–114.4	59.9–103.4	23.4–31.4%
300	1.8–11.0	80.0–161.7	78.2–150.7	13.0–18.5%
400	1.8–11.0	91.7–195.8	89.9–184.8	7.9–11.9%
500	1.8–11.0	99.4–220.8	97.6–209.8	15.8–22.7%
1000	1.8–11.0	117.7–282.4	115.9–271.4	

Estimates were determined as the difference in profile carbon storage in soils of different ages simulated with a nonlinear carbon accumulation model. Values represent estimates determined using minimum and maximum carbon accumulation scenarios.

position is determined as a fraction of carbon storage (equation (3)), as total carbon storage increases, the magnitude of carbon losses must also increase even through the decomposition coefficient (k) is decreasing. The model suggests that an approximate equilibrium (<5% difference from steady state) is reached within 650–800 years after fire. Since the current length of the fire cycle is much shorter than this (70–500 years), black spruce systems do not reach steady state and function as net carbon sinks over most of their life span. If fire severity remains constant, a reduction in the length of the fire cycle will result in a reduction of carbon storage potential. For example, a simulated increase in fire frequency from 300 to 200 years reduces soil carbon storage by 23–34% (Table 6). Due to the logarithmic shape of the carbon storage curve, the effect of fire on carbon storage is greatest in the first 200 years of ecosystem development. Should the length of time between fires decrease significantly, the ratio of time that soils serve as a net source of carbon to the time they function as a net sink will increase, resulting in a net loss of stored carbon from the system.

[41] At the same time, however, combustion introduces a large pulse of carbon-rich material to the soil surface [*Harmon et al.*, 1990; *Harden et al.*, 1997]. This material varies in its decomposability and may partially offset losses of carbon via decomposition. By reinitiating carbon accumulation and introducing a large pulse of carbon to the soil, fire may actually help perpetuate the role of boreal soils as sinks for carbon [*Harden et al.*, 1997, 2000].

[42] Extrapolation of this model over timescales longer than 200 years is limited by the lack of field data for validation. In most forest systems, NPP does not reach an equilibrium value, but begins to decline as the forest ages [*Waring and Running*, 1998]. Although total carbon uptake (gross primary productivity) does approach an equilibrium, plant respiration continues to increase as the amount of nonphotosynthetic tissue increases. As a result, extrapolation of the model beyond the 140 years represented by the chronosequence may overestimate carbon storage. However, because of the dominant role of mosses as a carbon input [*Viereck et al.*, 1983; *Goulden et al.*, 1998] and the long timescales over which these plants exhibit linear growth [*Clymo and Hayward*, 1982], reduction in NPP is likely to be less important than in temperate or tropical systems.

6. Conclusions

[43] CO_2 efflux from the soil surface increased logarithmically as a function of stand age to a maximum rate of 2.2 Mg C ha^{-1} yr^{-1} in a 140-year-old stand. This increase was highly correlated with the reestablishment of mosses and understory vegetation (R^2 = 0.89). Temporal patterns carbon accumulation based on field data indicate that rates of decomposition are enhanced by a factor of 3.5–4.75 in the first decade after fire when soil temperatures are elevated and then decline as soil temperatures cool and a plant canopy becomes reestablished. The net result of postfire changes in decomposition and carbon inputs results in a net accumulation of carbon in organic horizons on the order of 0.28–0.54 Mg C ha^{-1} yr^{-1}. A steady state carbon accumulation model modeling based on first-order kinetics suggests that these soils were a net source of carbon for 7–15 years after fire and released between 1.8 and 11.0 Mg C ha^{-1}, a potential loss of 12.4–12.6% of total soil organic matter. *Kasischke et al.* [2000a] found that fires in black spruce forests release between 10 and 76 Mg C ha^{-1}, with an average of 34 Mg C ha^{-1}. In some instances postfire emissions are on the same order of magnitude as the amount of CO_2 released during combustion itself and suggest the importance of incorporating postfire disturbance effects into regional carbon models.

[44] **Acknowledgments.** This work was funded by a National Aeronautics and Space Administration contract to Duke University and a NASA Earth Systems Sciences graduate fellowship. The equipment in this study was provided via a grant from ERIM International of Ann Arbor, MI. The authors wish to thank B. Custer, R. Nolen, J. McLain, and V. Krasovic for exceptional field assistance, P. Heine, B. Megonigal, W. Willis, and V. Jin for help with laboratory analyses, and M. Hofmockel for computer and other technical guidance. This manuscript benefited greatly from reviews and discussions with D. Ahmann (Colorado School of Mines), A. J. Shaw (Duke University), and J. Harden (USGS, Menlo Park) and suggestions from two anonymous reviewers.

References

Agriculture Canada Expert Committee on Soil Survey, *The Canadian System of Soil Classification*, 164 pp., Can. Govt. Publ. Cent., Ottawa, Canada, 1987.

Apps, M. J., W. A. Kurz, R. J. Luxmoore, L. O. Nilsson, R. A. Sedjo, R. Schmidt, L. G. Simpson, and T. S. Vinson, Boreal forests and tundra, *Water Air Soil Pollut.*, *70*, 39–53, 1993.

Auclair, A. N. D., and T. B. Carter, Forest wildfires as a recent source of CO_2 at northern latitudes, *Can. J. For. Res.*, *23*, 1530–1536, 1993.

Bonan, G. B., Soil temperature as an ecological factor in boreal forests, in *A Systems Analysis of the Global Boreal Forest*, edited by H. H. Shugart et al., pp. 126–143, Cambridge Univ. Press, New York, 1992.

Bonan, G. B., and K. Van Cleve, Soil temperature, nitrogen mineralization, and carbon source–sink relationships in boreal forests, *Can. J. For. Res.*, *22*, 629–639, 1991.

Bunnell, F. L., D. E. N. Tait, P. W. Flanagan, and K. Van Cleve, Microbial respiration and substrate weight loss, I, A general model of the influences of abiotic variables, *Soil Biol. Biochem.*, *9*, 3–40, 1977.

Burke, R. A., R. G. Zepp, M. A. Tarr, W. M. Miller, and B. J. Stocks, Effect of fire on soil–atmosphere exchange of methane and carbon dioxide in Canadian boreal forest sites, *J. Geophys. Res.*, *102*, 29,289–29,300, 1997.

Clymo, R. S., and P. M. Hayward, The ecology of *Sphagnum*, in *Bryophyte Ecology*, edited by A. J. E. Smith, pp. 229–289, Chapman and Hall, New York, 1982.

Dixon, R. K., S. Brown, R. A. Houghton, A. M. Solomon, M. C. Trexler, and J. Wisniewski, Carbon pools and flux in global forest ecosystems, *Science*, *263*, 185–190, 1994.

Dyrness, C. T., *Control of Depth to Permafrost and Soil Temperature by the Forest Floor in Black Spruce/Feathermoss Communities*, For. Serv. Res. Note PNW-396, 19 pp., U.S. Dept. of Agric., Pac. Northwest For. and Range Exp. Stn., Washington, D. C., 1982.

Flanagan, P. W., and K. Van Cleve, Microbial biomass, respiration, and nutrient cycling in a black spruce taiga ecosystem, in *Soil Organisms as Components of Ecosystems: International Soil Zoology Colloquium, Ecol. Bull.*, vol. 25, edited by U. Lohm and T. Persson, pp. 261–273, Swed. Nat. Sci. Res. Counc., Stockholm, 1977.

Flanagan, P. W., and A. K. Veum, Relationships between respiration, weight loss, temperature and moisture in organic residues on tundra, in *Soil Organisms and Decomposition in the Tundra*, edited by A. J. Holding et al., pp. 249–277, Tundra Biome Steering Committee, Stockholm, 1974.

Gorham, E., Northern peatlands: Role in the carbon cycle and probable responses to climate warming, *Ecol. Appl.*, *1*, 182–195, 1991.

Goulden, M. L., et al., Sensitivity of boreal forest carbon to soil thaw, *Science*, *279*, 214–217, 1998.

Harden, J. W., E. T. Sundquist, R. F. Stallard, and R. K. Mark, Dynamics of soil carbon during deglaciation of the Laurentide Ice Sheet, *Science*, *258*, 1921–1924, 1992.

Harden, J. W., K. P. O'Neill, S. E. Trumbore, H. Veldhuis, and B. J. Stocks, Moss and soil contributions to the annual net carbon flux of a maturing boreal forest, *J. Geophys. Res.*, *102*, 28,805–28,816, 1997.

Harden, J. W., S. E. Trumbore, B. J. Stocks, A. Hirsch, S. T. Gower, K. P. O'Neill, and E. S. Kasischke, The role of fire in the boreal carbon budget, *Global Change Biol.*, *6*(s1), 174–184, 2000.

Harmon, M. E., W. K. Ferrell, and J. F. Franklin, Effects on carbon storage of conversion of old-growth forests to young forests, *Science*, *247*, 699–702, 1990.

Jenny, H., S. Gessell, and F. T. Bingham, Comparative study of decomposition rates of organic matter in temperate and tropical regions, *Soil Sci.*, *68*, 419–432, 1949.

Johnson, D., L. Kershaw, A. MacKinnon, and J. Poplar, *Plants of the Western Boreal Forest and Aspen Parkland*, Lone Pine, Alberta, Can., 1995

Kasischke, E. S., The role of boreal ecosystems in the global carbon cycle, in *Fire, Climate Change, and Carbon Cycling in the North American Boreal Forest, Ecol. Stud. Ser.*, edited by E. S. Kasischke and B. J. Stocks, pp. 15–23, Springer-Verlag, New York, 2000.

Kasischke, E. S., N. H. F. French, L. L. Borgeau-Chavez, and N. L. Christensen Jr., Estimating release of carbon from 1990 and 1991 forest fires in Alaska, *J. Geophys. Res.*, *100*, 2941–2951, 1995.

Kasischke, E. S., K. P. O'Neill, N. H. F. French, and L. L. Borgeau-Chavez, Controls on patterns of biomass burning in Alaskan boreal forests, in *Fire, Climate Change, and Carbon Cycling in the North American Boreal Forest, Ecol. Stud. Ser.*, edited by E. S. Kasischke and B. J. Stocks, pp. 173–196, Springer-Verlag, New York, 2000a.

Kasischke, E. S., N. H. F. French, K. P. O'Neill, D. D. Richter, L. L. Borgeau-Chavez, and P. A. Harrell, Influence of fire on long-term patterns of forest succession in Alaskan boreal forests, in *Fire, Climate Change, and Carbon Cycling in the North American Boreal Forest, Ecol. Stud. Ser.*, edited by E. S. Kasischke and B. J. Stocks, pp. 214–235, Springer-Verlag, New York, 2000b.

Mackay, J. R., Active layer changes (1968–1993) following the forest–tundra fire near Inuvik, NWT, Canada, *Arct. Alp. Res.*, *27*, 323–326, 1995.

MacLean, D. A., S. J. Woodley, M. G. Weber, and R. W. Wein, Fire and Nutrient Cycling, in *The Role of Fire in the Northern Circumpolar Ecosystem (SCOPE 18)*, edited by R. W. Wein and D. A. MacLean, pp.11–132, John Wiley, New York, 1983.

Marion, G. M., and W. C. Oechel, Mid- to late-Holocene carbon balance in Arctic Alaska and its implications for future global warming, *Holocene*, *3*, 193–200, 1993.

O'Neill, K. P., Changes in carbon dynamics following wildfire in soils of interior Alaska, Ph.D. thesis, Duke Univ., Durham, 2000.

O'Neill, K. P., J. W. Harden, and S. E. Trumbore, *Boreal-Ecosystem Atmosphere Study (BOREAS): 1993 Laboratory Data and Notes*, USGS OFR 95-565, Thompson, Manitoba, 1995.

Olson, J. S., Energy storage and the balance of producers and decomposers in ecological systems, *Ecology*, *44*, 322–331, 1962.

Parkinson, K. J., An improved method for measuring soil respiration in the field, *J. Appl. Ecol.*, *18*, 221–228, 1981.

Rapalee, G., S. E. Trumbore, E. A. Davidson, J. W. Harden, and H. Veldhuis, Soil carbon stocks and their rates of accumulation and loss in a boreal forest landscape, *Global Biogeochem. Cycles*, *12*(4), 687–701, 1998.

Richter, D. D., K. P. O'Neill, and E. S. Kasischke, Stimulation of soil respiration in burned black spruce (*Picea mariana* L.) forest ecosystems: A hypothesis, in *Fire, Climate Change, and Carbon Cycling in the North American Boreal Forest*, edited by E. S. Kasischke and B. J. Stocks, pp. 164–178, Springer-Verlag, New York, 2000.

Schimel, J. P., and J. Gulledge, Microbial community structure and global trace gases, *Soil Biota Global Change*, *4*, 745–758, 1998.

Schlentner, R. E., and K. Van Cleve, Relationships between CO_2 evolution from soil, substrate temperature, and substrate moisture in four mature forest types in interior Alaska, *Can. J. For. Res.*, *15*, 97–106, 1985.

Schlesinger, W. H., Evidence from chronosequence studies for a low carbon-storage potential of soils, *Nature*, *348*, 232–234, 1990.

Schoephorster, D. B., *Soil Survey of Salcha-Big Delta Area, Alaska*, 51 pp., USDA Soil Conservation Service, Washington, D. C., 1973.

Schumacher, F. X., and R. A. Chapman, *Sampling Methods in Forestry and Range Management*, For. Sch. Bull. 7, 222 pp., Duke Univ., Durham, NC, 1954.

Singh, J. S., and S. R. Gupta, Plant decomposition and soil respiration in terrestrial ecosystems, *Bot. Rev.*, *43*, 449–528, 1977.

Stocks, B. J., M. A. Fosberg, M. B. Wotton, T. J. Lynham, and K. C. Ryan, Climate change and forest fire activity in North American boreal forests, in *Fire, Climate Change, and Carbon Cycling in the North American Boreal Forest*, edited by E. S. Kasischke and B. J. Stocks, pp. 312–319, Springer-Verlag, New York, 2000.

Swanson, D. K., Susceptibility of permafrost soils to deep thaw after forest fires in interior Alaska, U.S.A., and some ecologic implications, *Arct. Alp. Res.*, *28*, 217–227, 1996.

Tarnocai, C., and S. C. Zoltai, Earth hummocks of the Canadian Arctic and Subarctic, *Arct. Alp. Res.*, *10*, 581–594, 1978.

Tolonen, K., H. Vasander, A. W. H. Danman, and R. S. Clymo, Rate of apparent and true carbon accumulation in boreal peatlands, in *Proc. Int. Peat Congr., 9th, June 22–26, Uppsala Sweden*, pp. 319–333, Int. Peat Soc., Jyska, Finland, 1992.

Trettin, C. C., M. F. Jurgensen, M. R. Gale, and J. McLaughlin, Soil carbon in northern forested wetlands: Impact of silvicultural practices, in *Carbon Forms and Functions in Forest Soils*, edited by W. W. McFee and J. M. Kelly, pp. 437–461, Soil Sci. Soc. Am., Madison, Wisc., 1995.

Trumbore, S. E., and J. W. Harden, Accumulation and turnover of carbon in organic and mineral soils of the BOREAS northern study area, *J. Geophys. Res.*, *102*, 28,817–28,830, 1997.

Tryon, P. R., and F. S. Chapin III, Temperature control over root growth and root biomass in taiga forest trees, *Can. J. For. Res.*, *13*, 827–833, 1983.

United States Department of Agriculture, Natural Resources Conservations Service, 325 pp., *Keys to Soil Taxonomy (8th Edition)*, Pocáhontas Press, Blacksburg, Va., 1998.

Van Cleve, K., R. Barner, and R. Schlentner, Evidence of temperature control of production and nutrient cycling in two interior Alaska black spruce ecosystems, *Can. J. For. Res.*, *11*, 258–273, 1981.

Van Cleve, K., and J. Yarie, Interaction of temperature, moisture, and soil chemistry in controlling nutrient cycling and ecosystem development in the Alaskan taiga, in *Forest Ecosystems in the Alaskan Taiga*, edited by K. Van Cleve et al., pp. 160–189, Springer-Verlag, New York, 1986.

Van Cleve, K., L. K. Oliver, P. Schlentner, L. A. Viereck, and C. T. Dyrness, Productivity and nutrient cycling in taiga forest ecosystems, *Can. J. For. Res.*, *13*, 703–720, 1983.

Veldhuis, H., and D. Knapp, *BOREAS TE-20 NSA Soil Lab Data Set*, Distrib. Active Arch. Cent., Oak Ridge Natl. Lab., Oak Ridge, Tenn., 1998. (Available at http://www.eodis.ornl.gov/).

Viereck, L. A., Forest ecology of the Alaskan taiga, *Quat. Res.*, *3*, 465–495, 1975.

Viereck, L. A., Effects of fire and firelines on active layer thickness and soil temperatures in interior Alaska, in *Proceedings 4th Canadian Permafrost Conference, Calgary, Alberta*, pp. 123–135, Natl. Res. Counc. of Can., Ottawa, March 2–6, 1982.

Viereck, L. A., C. T. Dyrness, K. Van Cleve, and M. J. Foote, Vegetation, soils, and forest productivity in selected forest types in interior Alaska, *Can. J. For. Res.*, *13*, 703–720, 1983.

Waring, R. H., and S. W. Running (eds.), *Forest Ecosystems: Analysis at Multiple Scales*, 370 pp., Academic, San Diego, Calif., 1998.

Wein, R. W., Frequency and characteristics of arctic tundra fires, *Arctic*, *29*, 213–222, 1976.

Wein, R. W., and L. C. Bliss, Changes in arctic Eriophorum tussock communities following fire, *Ecology*, *54*, 845–852, 1973.

Whalen, R. J., *The Ecology of Fire*, 346 pp., Cambridge Univ. Press, New York, 1995.

Winston, G. C., E. T. Sundquist, B. B. Stephens, and S. E. Trumbore, Winter CO_2 fluxes in a boreal forest, *J. Geophys. Res.*, *102*, 28,795–28,804, 1997.

Wotton, B. M., and M. D. Flannigan, Length of fire season in a changing climate, *For. Chron.*, *69*, 187– 192, 1993.

E. S. Kasischke, Department of Geography, University of Maryland, College Park, MD, USA.

K. P. O'Neill, North Central Research Station, USDA Forest Service, 1992 Folwell Avenue, St. Paul, MN 55108, USA. (koneill@fs.fed.us)

D. D. Richter, Nicholas School of the Environment, Duke University, Durham, NC 27708-0328, USA.